



Modeling the adsorption of Cr(III) from aqueous solution onto *Agave lechuguilla* biomass: Study of the advective and dispersive transport

J. Romero-González^{a,*}, J.C. Walton^{b,d}, J.R. Peralta-Videa^c, E. Rodríguez^a, J. Romero^d, J.L. Gardea-Torresdey^b

^a Instituto de Ingeniería y Tecnología, Universidad Autónoma de Ciudad Juárez, Av. Del Charro No. 610 Norte, Cd. Juárez, Chihuahua 32310 México, Mexico

^b Environmental Science and Engineering Ph.D. Program, University of Texas at El Paso, El Paso, TX 79968, USA

^c Department of Chemistry, University of Texas at El Paso, El Paso, TX 79968, USA

^d Civil Engineering Department, University of Texas at El Paso, El Paso, TX 79968, USA

ARTICLE INFO

Article history:

Received 8 December 2005

Received in revised form 23 March 2008

Accepted 25 March 2008

Available online 30 March 2008

Keywords:

Model

Chromium (III)

Adsorption

Agave lechuguilla

Packed column

ABSTRACT

The biosorption of Cr(III) onto packed columns of *Agave lechuguilla* was analyzed using an advective–dispersive (AD) model and its analytical solution. Characteristic parameters such as axial dispersion coefficients, retardation factors, and distribution coefficients were predicted as functions of inlet ion metal concentration, time, flow rate, bed density, cross-sectional column area, and bed length. The root-mean-square-error (RMSE) values 0.122, 0.232, and 0.285 corresponding to the flow rates of 1, 2, and 3 (10⁻³) dm³ min⁻¹, respectively, indicated that the AD model provides an excellent approximation of the simulation of lumped breakthrough curves for the adsorption of Cr(III) by lechuguilla biomass. Therefore, the model can be used for design purposes to predict the effect of varying operational conditions.

© 2008 Published by Elsevier B.V.

1. Introduction

The treatment of high volumes of wastewater containing low concentrations of pollutants is becoming increasingly important as discharge regulations become more stringent. The treatment and disposal of liquid effluents from leather tanning and textile industries are a serious problem due to their Cr(III) contents [1,2]. Although Cr(III) is less toxic than Cr(VI), a cancer-causing agent, Cr(III) may be a toxic metal when present at high concentrations [3–5]. The treatments applied towards the removal of Cr(III) involve physicochemical processes such as coagulation and precipitation [6]. However these techniques proved ineffective in remaining within Cr(III) discharge limits (1–2 mg/dm³) of industrial effluents [7]. As a result, the use of alternative treatments such as ion exchange, carbon adsorption, membrane filtration, electroseparation, and bioaccumulation has been applied in “polishing” these effluents [8–10]. However, such processes may be ineffective and extremely expensive. Bioadsorption, on the other hand, is an emerging technology that also works to overcome the selectivity disadvantages of traditional decontamination processes [11,12]. Table 1 shows the comparative factors

of effluent decontamination methods. The bioadsorption process offers the advantages of low operating cost, volume minimization of chemical and/or biological sludge to be disposed of, high efficiency for contaminant removal, and no nutrient requirements as needed in bioaccumulation processes. Several materials that are available in large quantities, such as industrial, agricultural, or natural waste products, have been prospected as bioadsorbents of Cr(III) such as humic acids [13], alfalfa [14], cork powder [15], and brown seaweed [16]. *Agave lechuguilla*, generally known as lechuguilla, has been identified as a potential prospective biomass that can be used in the removal of trivalent chromium [17,18]. Lechuguilla is used for several purposes such as syrup and alcoholic beverage production, and fabrication of goods from fibers [19]. Additionally, its roots and leaves contain active chemicals such as saponins and steroids (25R)-spirost-5-ene-2 alpha, 3 beta-diol (yuccagenin) and (25R)-5 beta-spirostane-3 beta, 6 alpha-diol (ruizgenin) which are used in medicinal applications [20]. During such processes high quantities of waste that remain rich in cellulose are produced. These characteristics make lechuguilla a cheap source of biomaterial for the removal of heavy metals from water and wastewater. Recently, researches have shown that saponins can be used as natural chelating agents to remove heavy metals such as Cr, Cd, Cu, Pb, and Zn from diverse environments [21,22]. These physical and chemical properties of lechuguilla support its potential application and possible high capacity to remove

* Corresponding author. Tel.: +52 656 6884800; fax: +52 656 6884800.
E-mail address: jromero@uacj.mx (J. Romero-González).

Nomenclature

A	cross-sectional area (dm^2)
A_{Ad}	reduction area (mg min dm^{-1})
C_{Ad}	bed reduction capacity (mg g^{-1})
C_0	input metal ion concentration (mg dm^{-3})
D	axial dispersion coefficient ($\text{dm}^2 \text{min}^{-1}$)
K_d	distribution coefficient ($\text{dm}^3 \text{mg}^{-1}$)
Q	flow rate ($\text{dm}^{-3} \text{min}^{-1}$)
R	retardation factor
t	time (min)
U_0	average approach velocity
W	mass of adsorbent (g)
z	column bed length (dm)

Greek symbols

ε	porosity
γ	zero-order liquid phase source
μ	general first-order decay constant (min^{-1})
ρ_{ads}	density (mg dm^{-3})
τ	residence time (min)
ν	pore water velocity, $\nu = Q/A\varepsilon$ (dm min^{-1})

heavy metals from aqueous solution using packed column systems [23].

Several important challenges involved in the actual application of bioadsorption include the selectivity of bioadsorbents and the development of a continuous process. The application of predictive and simulative mathematical models for the design of equipment in biosorptive metal uptake represents an important area in environmental engineering [24–26]. These models can economize time and effort involved in designing treatment systems for water and wastewater. The determination of model parameters and the verification of model validity may be achieved by a well-designed set of experiments. The purpose of mathematical modeling is to reduce the scope and magnitude of pilot-scale studies and to design full-scale processes [24–28,30,31]. Models can be developed combining the mass balances with the equilibrium constants of the supposed active site-ion interaction. Using this procedure, mathematical equations relating equilibrium metal concentration in solid and liquid phase can be carried out under such experimental conditions as concentration, time, and pH. The equilibrium values of the supposed interaction or reactions are the adjustable parameters of these models determined by linear or non-linear methods [24,32,30]. In addition, the performance of dynamic sorption column systems requires simultaneous considerations of changes of sorption equilibrium, sorbate solution chemistry, bioadsorption mechanism, mass transfer, and fluid-flow rate. All these parameters determine the overall sorption performance and the shape of the column breakthrough curves [31–33]. This study discusses the

development and application of an analytical method for modeling Cr(III) adsorption by lechuguilla biomass in packed column systems to determine characteristic parameters and the effect of dynamic operation conditions in the adsorption process, both of which are useful for process design. Also, the use of these parameters generated by the model can be developed to describe the mechanism of Cr adsorption.

2. Materials and methods

Inactive tissues of lechuguilla plants were collected around the city of El Paso, Texas, USA. The debris and soil of collected tissues were removed by using abundant tap water. Only the leaves of the plants were utilized in this study since they represent more than 90% of lechuguilla plants. After washing, the leaves were oven dried at 80 °C for 72 h and ground to pass through a 0.150 mm sieve using a Wiley mill. A stock solution of 4 mg dm^{-3} of Cr(III) was prepared by dissolving a weighed quantity of $\text{Cr}(\text{NO}_3)_3$ in deionized water. The pH of the influent solution and biomass was adjusted to pH 4 using diluted solutions of HCl and NaOH. This pH value was found to be the optimal pH for Cr(III) biosorption in previous batch studies [17,18]. Column experiments were performed in glass columns of 0.07 dm of internal diameter. The biomass was packed to a bulk density (mass of adsorbent in a specific volume) of 6.52 (10^5) mg dm^{-3} to get bed lengths of 0.5, 1, and 1.5 dm, respectively. The bed porosity, ε , was determined as the volume of deionized water required to fill the porous of the dry bed (V_w) in the respective bed volume (V_b), $\varepsilon = V_w/V_b \text{ dm}^3 \text{ dm}^{-3}$. The column experiments were carried out at room temperature (22 °C) and with control set to pH 4 during the experiments in triplicate. The solution was fed to the top of the column by a Masterflex pump (Cole-Parmer Model 7524) and the effluents were taken at intervals of 6, 3, and 2 min with a fraction collector (Spectra/Chrom CF-1) at the influent flow rates of 1, 2, and 3 (10^{-3}) $\text{dm}^3 \text{min}^{-1}$, respectively. The Cr content in effluent and influent was determined by using an inductively coupled plasma optical emission spectrophotometer (ICP-OES) (PerkinElmer Optima 4300 DV). The ICP-OES operation conditions were: emission line 283.563 nm; detection limit 0.01 mg dm^{-3} ; radio frequency power 1450 W.

3. Model description

The breakthrough curves and mass transfer zone of a flow-through fixed-bed biosorption column are of great importance. The fixed-bed model based on the assumption of a constant breakthrough pattern through the bed is quite reasonable. But there are three different zones within the fixed-bed processes including the saturated zone, mass transfer zone, and blank zone. The modeling of the mass transfer zone behavior under variable conditions in a flow-through fixed-bed sorption column enabled the prediction of breakthrough curves [33]. The mass balance on the adsorbate in the mass transfer zone of an adsorption column without chemical

Table 1
Methods for chromium effluent decontamination

Method	Selectivity	Flow rates	Concentrations	pH range	Capital cost	Waste material production	Energy consumption per m^3 of effluent (kWh)
Neutralization-precipitation	Low	High	High	Low	High	Very high	2.1–3.7
Ion exchange	High	Low	Low	Low	Low	Low	0.3
Activated charcoal adsorption	Low	Low	Low	Low	Low	Low	0.3
Separation by membrane	Low	Low	Low	High	High	Low	2.1–2.6
Electroseparation	High	High	High	Low	Very high	Low	2–10
Microbial metal sorption	High	Low	Low	Low	Low	Low	0.3
Biosorption	High	Low	Low	High	Very low	Low	0.3

Information obtained from [11,12,46].

reaction is expressed as follows [31]:

$$\frac{\partial c}{\partial t} = -\frac{U_0}{\varepsilon} \frac{\partial c}{\partial z} + D \frac{\partial^2 c}{\partial z^2} - \frac{\rho_{\text{ads}}(1-\varepsilon)}{\varepsilon} \frac{\partial q}{\partial t} \quad (1)$$

where ε represents porosity; D is the axial dispersion coefficient for the adsorbate; U_0 is the average approach velocity of the metal aqueous solution, and ρ_{ads} is the density of the adsorbent particles.

In models such as the Adams–Bohart and Clark models, which were originally developed for gas–charcoal (gas and solid phases) adsorption systems, the dispersion is considered negligible when compared to advection and adsorption in the removal of the adsorbate from aqueous solutions [34,35]. Thus, Eq. (1) is usually simplified as follows:

$$\frac{\partial c}{\partial t} = -\frac{U_0}{\varepsilon} \frac{\partial c}{\partial z} - \frac{\rho_{\text{ads}}(1-\varepsilon)}{\varepsilon} \frac{\partial q}{\partial t} \quad (2)$$

However, in the present study we used Eq. (1) as originally defined, because the axial dispersion coefficient, D , makes the model applicable in cases in which the transfer resistances are present in the liquid and solid phases [36,37].

$$A(z, t) = \frac{(v) \operatorname{erfc}\left(\frac{zR-ut}{\sqrt{4DRt}}\right) \exp\left(\frac{(v-u)z}{2D}\right)}{(v+u)} + \frac{(v) \operatorname{erfc}\left(\frac{zR+ut}{\sqrt{4DRt}}\right) \exp\left(\frac{(v+u)z}{2D}\right)}{(v-u)} + \frac{(v^2) \operatorname{erfc}\left(\frac{zR+ut}{\sqrt{4DRt}}\right) \exp\left(\frac{zv}{D} - \frac{t\mu}{R}\right)}{2\mu D} \quad (13)$$

$$B(z, f) = \left(\frac{y}{\mu} - Ci\right) \left(\frac{\operatorname{erfc}\left(\frac{zR-ut}{\sqrt{4DRt}}\right) \left(\frac{v^2t}{DR} + \frac{zv}{D} + 1\right) \exp\left(\frac{zv}{D}\right) \operatorname{erfc}\left(\frac{zR+ut}{\sqrt{4DRt}}\right)}{2} + \exp\left(-\frac{(zR-ut)^2}{4DRt}\right) \left(\sqrt{\frac{v^2t}{\pi DR}}\right) \right) \times \exp\left(-\frac{vt}{R}\right) + \frac{\gamma}{\mu} + \left(Ci - \frac{\gamma}{\mu}\right) \exp\left(\frac{t\mu}{R}\right) \quad (14)$$

The equilibrium distribution between the solid phase and the fluid phase can be described by a linear isotherm of the form [18,31]

$$q = K_d c \quad (3)$$

Then

$$\frac{\partial q}{\partial t} = K_d \frac{\partial c}{\partial t} \quad (4)$$

substituting Eq. (4) into Eq. (2), the following equation was obtained:

$$\left(1 + \frac{\rho_{\text{ads}}(1-\varepsilon)}{\varepsilon} K_d\right) \frac{\partial c}{\partial t} = -\frac{U_0}{\varepsilon} \frac{\partial c}{\partial z} + D \frac{\partial^2 c}{\partial z^2} \quad (5)$$

From there the general advective–dispersive equation can be written as follows:

$$R \frac{\partial c}{\partial t} = -v \frac{\partial c}{\partial z} + D \frac{\partial^2 c}{\partial z^2} \quad (6)$$

where the retardation factor R , a dimensionless parameter characterizing the retarding effect of adsorption on solute transport [29,32], is defined by:

$$R = \left(1 + \frac{\rho_{\text{ads}}(1-\varepsilon)}{\varepsilon} K_d\right) \quad (7)$$

and the pore velocity v is defined by:

$$v = \frac{U_0}{\varepsilon} \quad (8)$$

To find the most descriptive alternative with a minimum of operation variables for a successful theoretical treatment of experimental data and simulation of bioadsorption breakthrough curves, several analytical solutions of the advection–dispersion equation,

were analyzed [38–43]. After the analyses, the van Genuchten analytical solution [44] was selected to simulate the adsorption process.

The equations, conditions, and variables used were the following: Eq. (6) was solved using the following initial and boundary conditions:

$$c(z, 0) = Ci \quad (9)$$

$$\left(-D \frac{\partial c}{\partial z} + vc\right)_{z=0} = \begin{cases} vC_0 & 0 < t \leq t_0 \\ 0 & t > t_0 \end{cases} \quad (10)$$

$$\frac{\partial c}{\partial z}(\infty, t) = 0 \quad (11)$$

where C_i and C_0 are constants. The modified van Genuchten analytical solution using Laplace transforms is [40]:

$$c(z, t) = \begin{cases} (C_0 - \gamma/\mu)A(z, t) + B(z, t) & 0 < t \leq t_0 \\ (C_0 - \gamma/\mu)A(z, t) + B(z, t) - C_0A(z, t - t_0) & t > t_0 \end{cases} \quad (12)$$

where

$$A(z, t) = \frac{(v) \operatorname{erfc}\left(\frac{zR-ut}{\sqrt{4DRt}}\right) \exp\left(\frac{(v-u)z}{2D}\right)}{(v+u)} + \frac{(v) \operatorname{erfc}\left(\frac{zR+ut}{\sqrt{4DRt}}\right) \exp\left(\frac{(v+u)z}{2D}\right)}{(v-u)} + \frac{(v^2) \operatorname{erfc}\left(\frac{zR+ut}{\sqrt{4DRt}}\right) \exp\left(\frac{zv}{D} - \frac{t\mu}{R}\right)}{2\mu D} \quad (13)$$

$$B(z, f) = \left(\frac{y}{\mu} - Ci\right) \left(\frac{\operatorname{erfc}\left(\frac{zR-ut}{\sqrt{4DRt}}\right) \left(\frac{v^2t}{DR} + \frac{zv}{D} + 1\right) \exp\left(\frac{zv}{D}\right) \operatorname{erfc}\left(\frac{zR+ut}{\sqrt{4DRt}}\right)}{2} + \exp\left(-\frac{(zR-ut)^2}{4DRt}\right) \left(\sqrt{\frac{v^2t}{\pi DR}}\right) \right) \times \exp\left(-\frac{vt}{R}\right) + \frac{\gamma}{\mu} + \left(Ci - \frac{\gamma}{\mu}\right) \exp\left(\frac{t\mu}{R}\right) \quad (14)$$

and

$$u = v \sqrt{\frac{4\mu D}{v^2} + 1} \quad (15)$$

where μ is the first-order decay constant and γ is zero-order liquid phase source, which were considered close to zero because Cr(III) is non-reactive at the operation conditions of the system.

The root-mean-square-error (RMSE) between the experimental and predicted values is defined by:

$$\text{RMSE} = \sqrt{\frac{\sum((C_i)_{\text{experimental}} - (C_i)_{\text{predicted}})^2}{N}} \quad (16)$$

where N is the total number of data points.

To model the adsorption process, the van Genuchten analytical solution required the following variables.

- Operating conditions: C_0 , input metal ion concentration (mg dm^{-3}); t , time (min); Q , flow rate ($\text{dm}^{-3} \text{min}^{-1}$).
- Biosorbent physical properties: ρ_{ads} , density (mg dm^{-3});
- Column characteristics: internal diameter (dm), A , cross-sectional area (dm^2); ε , porosity; z , bed length column (dm); v , pore water velocity, $v = Q/A\varepsilon$ (dm min^{-1}).

The analytical solution generates the following design and scale up parameters:

- D , axial dispersion coefficient ($\text{dm}^2 \text{min}^{-1}$);
- R , retardation factor;
- K_d , distribution coefficient ($\text{dm}^3 \text{mg}^{-1}$);

The column studies were carried out on lechuguilla at various flow rates and bed packed lengths. In addition, column parameters for the model given by the van Genuchten's analytical solution (Eqs.

Table 2
Operational condition of the column experiments

Metal in influent	Cr(III)
Input concentration, C_0	4.0 mg dm^{-3}
Flow rates, Q	$1, 2, 3 (10^{-3}) \text{ dm}^3 \text{ min}^{-1}$
Lechuguilla particles density, ρ_{ads}	$8.7 (10^3) \text{ mg dm}^{-3}$
Column internal diameter	0.07 dm
Bed porosity, ϵ	0.25
Bed high column, z	$0.5, 1, 1.5 \text{ dm}$
pH	4

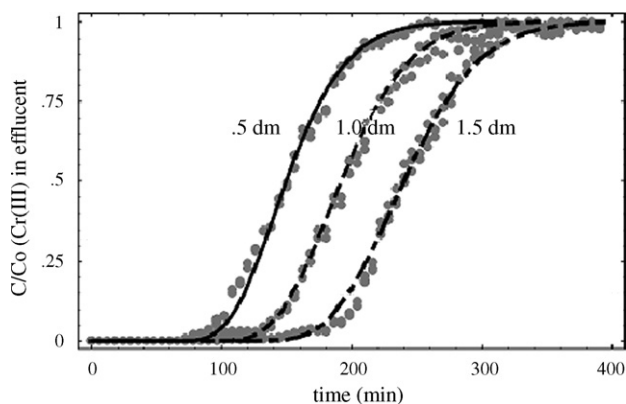


Fig. 1. Lumped breakthrough curves of Cr(III) sorption by lechuguilla biomass with the model. The model profiles are presented with different lines and the points denote experimental values at bed lengths, 0.5 (—), 1(---), 1.5(---) dm; flow rate, $10^{-3} \text{ dm}^3 \text{ min}^{-1}$; pH 4 and C_0 , 4 mg/dm^{-3} .

(12)–(16) were estimated from the Cr(III) column biosorption data by using a *Mathematica* 4.1 computer program (Wolfram Research, Inc.). Table 2 shows the operational condition used in these column experiments.

4. Results and discussion

4.1. Effect of bed high and flow rate

The simulation of the lumped breakthrough curves at 1, 2, and $3 (10^{-3}) \text{ dm}^3 \text{ min}^{-1}$ flow rates are shown in Figs. 1–3, respectively. As seen in these figures, the comparison of model estimated data (lines) with experimental concentration profiles (points) of Cr(III) proves that the model is an appropriate tool to assist with interpretation of the experimental results and simulate the process.

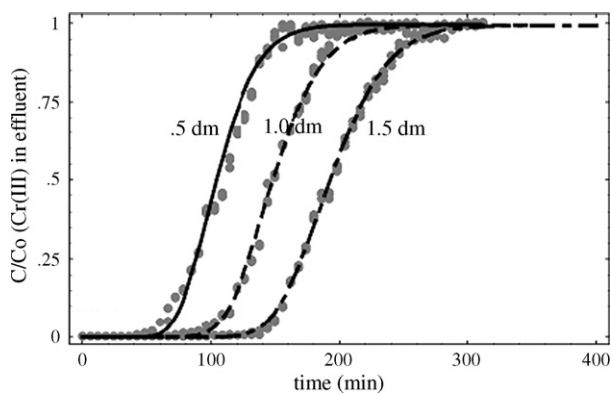


Fig. 2. Lumped breakthrough curves of Cr(III) sorption by lechuguilla biomass with the model. The model profiles are presented with different lines and the points denote experimental values at bed lengths, 0.5 (—), 1(---), 1.5(---) dm; flow rate, $2 (10^{-3}) \text{ dm}^3 \text{ min}^{-1}$; pH 4 and C_0 , 4 mg/dm^{-3} .

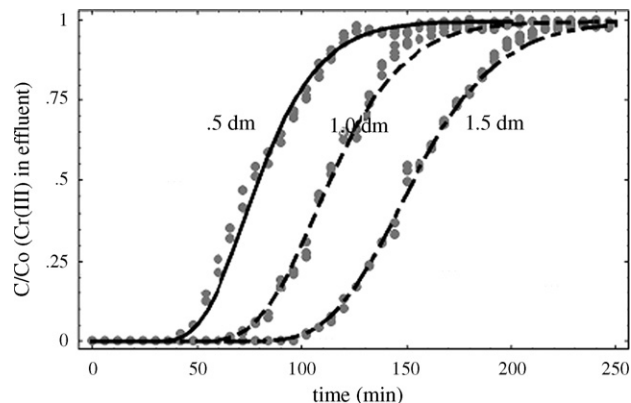


Fig. 3. Lumped breakthrough curves of Cr(III) sorption by lechuguilla biomass with the model. The model profiles are presented with different lines and the points denote experimental values at bed lengths, 0.5 (—), 1(---), 1.5(---) dm; flow rate, $3 (10^{-3}) \text{ dm}^3 \text{ min}^{-1}$; pH 4 and C_0 , 4 mg/dm^{-3} .

Figs. 1–3 show that for short times Cr(III) feed is taken up completely by the column. After a while chromium breakthrough occurs and the effluent concentration increases with time. In the studies performed the pH did not change at the end of the column throughout the experiment. It is normal practice in column operations to terminate the influent flow at the breakthrough time (t_b) at which the contaminant reaches a specified concentration, C_b . So as observed in Figs. 1–3, the increase in the breakthrough point (t_b), time at 50% of breakthrough (C_b equals to 0.5 of C/C_0), is directly dependent of the bed high column and inversely dependent of the flow rate. In other words, the t_b at a constant flow rate of $1 (10^{-3}) \text{ dm}^3 \text{ min}^{-1}$ for bed length of 0.5, 1, and 1.5 dm were 148, 193, and 242 min, respectively. On the other hand, Figs. 1–3 showed that t_b at a constant high bed of 1 dm for a flow rate of 1, 2, and $3 (10^{-3}) \text{ dm}^3 \text{ min}^{-1}$ were 193, 149, 118 min, respectively.

4.2. Relationship between the adsorption capacity and residence times

For the practical design of packed columns, the factors of operation, with respect to the adsorbent and to the fluid phase, must be defined. In connection with the time of operation, these factors are a suitable basis for the design of adsorbent systems [44,45,25]. Therefore, the bed adsorption capacities of lechuguilla for Cr(III) were estimated from the simulated breakthrough curves (at 50% of breakthrough point) and the mean residence times, τ (min), defined by Eq. (17):

$$\tau = \frac{V}{Q} = \frac{Az}{Q} = \frac{z}{U_0} \tag{17}$$

where V is the column bed volume (dm^3), A is the cross-sectional area (dm^2), z is bed length column (dm), Q is the flow rate of the influent ($\text{dm}^3 \text{ min}^{-1}$), and U_0 is the average approach velocity of the metal aqueous solution (dm min^{-1}).

The column adsorption capacities of lechuguilla were estimated from the adsorption areas generated by the model, A_{Ad} (mg min dm^{-3}), for each set of experiments. The adsorption capacities were calculated using the following equation:

$$C_{\text{Ad}} = \frac{A_{\text{Ad}}Q}{W} \tag{18}$$

where C_{Ad} is the bed adsorption capacity (mg g^{-1}), Q is the flow rate ($\text{dm}^3 \text{ min}^{-1}$), and W (g) is the mass of adsorbent at the respective bed length, z (dm). Fig. 4 shows an example of this process.

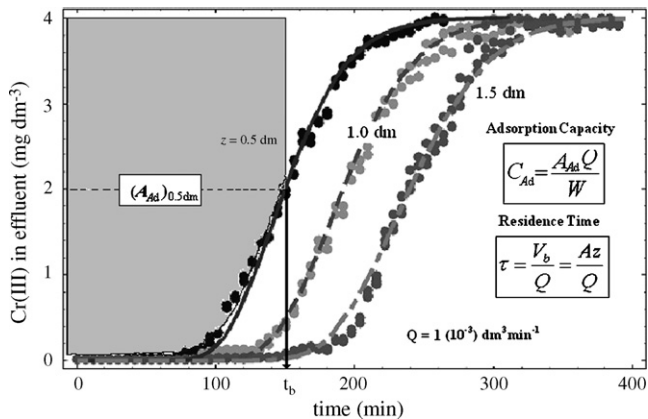


Fig. 4. Process to estimate the adsorption capacities and residence times of columns from the lumped breakthrough curves of Cr(III) sorption by lechuguilla biomass.

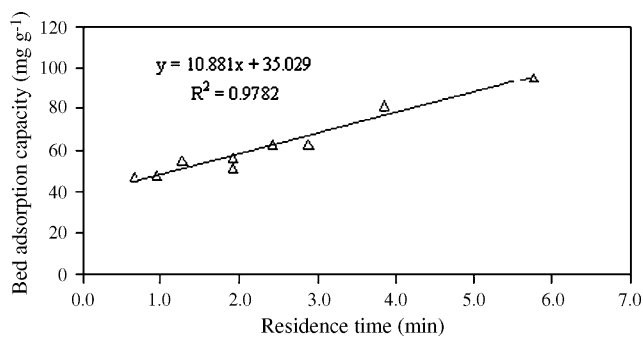


Fig. 5. Residence times vs. bed adsorption capacities for lechuguilla at pH 4.

These two parameters were determined for the different operational conditions. Fig. 5 shows the relationship between bed adsorption capacities and the residence times at pH 4, which is the optimal for the adsorption of Cr(III) by lechuguilla [17,18]. At low residence times, a low adsorption capacity occurred. While at high residence times the adsorption capacity increased. As seen in Fig. 5, at a residence time of 1 min the adsorption capacity was 42 mg g^{-1} . However, at a residence time of 6 min the adsorption capacity was 95 mg g^{-1} .

Also as shown in Fig. 4, the bed adsorption capacity is proportional to the metal solution residence time in the bed ($R^2 = 0.9782$), which indicates that the calculated relationship can be used to the desired level by designing a packed column of appropriate cross-sectional area and height.

In addition, the results showed that the highest adsorption capacity for lechuguilla packed columns was 95 mg g^{-1} , similar value reported for chitosan, 92 mg g^{-1} [46]. But it was higher than the values reported with other biomass packed column systems such as sphagnum peat moss, 29 mg g^{-1} , or peat, 76 mg g^{-1} [46].

4.3. Model parameters

Table 3 shows the design parameters generated from the model; these results showed that an increase in flow rate (from 1 to 3

Table 3
Model parameters corresponding to experimental conditions

Q ($10^{-3} \text{ dm}^3 \text{ min}^{-1}$)	D ($\text{dm}^2 \text{ min}^{-1}$)	Retardation	K_d ($10^{-5} \text{ dm}^3 \text{ mg}^{-1}$)	RMSE
1	0.021	200	7.27	0.122
2	0.022	154	5.47	0.232
3	0.032	118	4.00	0.285

(10^{-3}) $\text{dm}^3 \text{ min}^{-1}$) decreases the retardation factor (from 200 to 118) without a significant change of the axial dispersion coefficient (from 0.021 to $0.032 \text{ dm}^2 \text{ min}^{-1}$). Similar patterns were reported for the adsorption of a cationic surfactant using agricultural soil columns [47], transport of Copper and Cadmium in lateritic silty-clay soil columns [29], Nitrate adsorption in Fe^0 -packed columns [48], and Cr(VI) adsorption onto lechuguilla biomass columns [23]. The results of the present study suggest that Cr(III) adsorption in lechuguilla packed columns is instantaneous and that axial dispersion is not negligible and the initial slope of the breakthrough curve may be due to the retarding effect of adsorption on solute transport [32,33,49].

The different K_d values obtained (Table 3), depending on the operating conditions in adsorption column process, showed similar behavior of these results as reported in other works that indicate that in a dynamics system, like an adsorption packet column, the solute transport and adsorption depend on the fluidodynamic conditions [30,47,49]. Also previous equilibrium, kinetic and thermodynamic studies of Cr(III) adsorption from aqueous solutions by *A. lechuguilla* biomass demonstrated that at pH 4 the binding pattern for Cr(III) followed a linear and Langmuir isotherm and that its adsorption was not time-dependent (instantaneous) without any intraparticle resistance [17,18].

The integral analysis of these results suggest that Cr(III) adsorption takes place in the external surface of the lechuguilla biomass. This further supports the results of our previous studies that suggest that the binding of Cr(III) may be caused by interactions with functional groups such as carboxyl groups located on the surface of the cell tissue of the bioadsorbent [14,17,18,50,51]. In addition, the RMSE < 0.3 values indicated that the AD model and its analytical solution provided a close approximation of the simulation of the adsorption of Cr(III) by lechuguilla. Therefore, the model can be used for design purposes to predict the effect of varying operation conditions.

5. Conclusions

This study shows that *A. lechuguilla* can be used effectively for continuous bioadsorption of Cr(III) from aqueous solution. In addition, the experimental data and calculated design parameters suggest that Cr(III) adsorption takes place in the external surface of the lechuguilla biomass. Moreover, the model development can be efficiently used to represent the adsorption of Cr(III) from aqueous solutions using *A. lechuguilla* biomass in packed column systems; therefore, this development can potentially be applied to whichever reactive solutes using different biomasses. The analytical solution of the proposed model can also be applied to simulate the whole breakthrough curves in order to determine the scale up parameters of packed columns using all variables that constitute the advective and dispersive transport of removal of metals from aqueous solution onto biomass.

Acknowledgements

The authors would like to acknowledge financial support from the National Institutes of Health (NIH) (Grant S06GM8012-33) and the University of Texas at El Paso's Center for Environmental Resource Management (Cooperative agreement CR-819849-01-04) through funding from the Office of Exploratory Research of the EPA. In addition, the authors acknowledge the financial assistance from HBCU/MI ETC that is funded by the Department of Energy. Dr. Gardea-Torresdey acknowledges the funding from the National Institute of Environmental Health Sciences (Grant R01ES11367-01).

References

- [1] C.P. Jordao, J.L. Pereira, G.N. Jham, Chromium contamination in sediment, vegetation and fish caused by tanneries in the State of Minas Gerais, Brazil, *Sci. Total Environ.* 207 (1997) 1–11.
- [2] J. Kotaš, Z. Stasicka, Chromium occurrence in the environment and methods of its speciation, *Environ. Pollut.* 107 (2000) 263–283.
- [3] World Health Organization, Chromium in Drinking-water, Guidelines for drinking-water quality, Second ed., Geneva, 1993, pp. 45–55.
- [4] A.R. Walsh, J. O'Halloran, Chromium speciation in tannery effluent-II. Speciation in the effluent and in a receiving estuary, *Water Res.* 30 (1996) 2401–2412.
- [5] J. Blasiak, J. Kowalik, A comparison of the in vitro genotoxicity and tri- and hexavalent chromium, *Mutat. Res. Genet. Toxicol. Environ. Mutagen.* 469 (2000) 135–145.
- [6] J. Landgrave, A pilot plant for removing chromium residual waters of tanneries, *Environ. Health Perspect.* 103 (1989) 63–65.
- [7] M.S. El-Geundi, Adsorbents for industrial pollution control, *Adsorpt. Sci. Technol.* 15 (1997) 777–787.
- [8] M.M. Alves, C.G. González Beça, R. Guedes de Carvalho, J.M. Castanheira, M.C. Sol Pereira, L.A.T. Vasconcelos, Chromium removal in tannery wastewaters "polishing" by *Pinus sylvestris* bark, *Water Res.* 27 (1993) 1333–1338.
- [9] J. Jangbarwala, Ion exchange resins for metal finishing wastes, *Met. Finish.* 95 (1997) 33–34.
- [10] R.F. Unz, K.L. Shuttleworth, Microbial mobilization and immobilization of heavy metals, *Curr. Opin. Biotechnol.* 7 (1996) 307–310.
- [11] I. Gaballah, G. Kilbertus, Recovery of heavy metal ions through decontamination of synthetic solutions and industrial effluents using modified barks, *J. Geochem. Explor.* 62 (1998) 241–286.
- [12] B. Volesky, Detoxification of metal-bearing effluents: biosorption for the next century, *Hydrometallurgy* 59 (2001) 203–216.
- [13] M. Fukushima, K. Nakayasu, S. Tanaka, H. Nakamura, Chromium (III) binding abilities of humic acids, *Anal. Chim. Acta* 317 (1995) 195–206.
- [14] J.L. Gardea-Torresdey, K. Dokken, K.J. Tiemann, J.G. Parsons, J. Ramos, N.E. Pingitore, G. Gamez, Infrared and X-ray adsorption spectroscopic studies on the mechanism of chromium (III) binding to alfalfa biomass, *Microchem. J.* 71 (2002) 157–166.
- [15] R. Machado, J.R. Carvalho, M.J.N. Correia, Removal of trivalent chromium (III) from solution by biosorption in cork powder, *J. Chem. Technol. Biotechnol.* 77 (2002) 1340–1348.
- [16] Y. Yun, D. Park, J.M. Park, B. Volesky, Biosorption of trivalent chromium on the brown seaweed biomass, *Environ. Sci. Technol.* 35 (2001) 4353–4358.
- [17] J. Romero-González, J.R. Peralta-Videa, E. Rodríguez, M. Delgado, J.L. Gardea-Torresdey, Potential of *Agave lechuguilla* biomass for Cr(III) removal from aqueous solutions: thermodynamic studies, *Bioresour. Technol.* 97 (2006) 178–182.
- [18] J. Romero-González, J.L. Gardea-Torresdey, J.R. Peralta-Videa, E. Rodríguez, Determining the equilibrium and kinetic parameters of the Cr(VI) and Cr(III) adsorption from aqueous solutions by *Agave lechuguilla* biomass, *Bioinorg. Chem. Appl.* 3 (2005) 55–68.
- [19] H.S. Gentry, *Agaves of Continental North America*, The University of Arizona Press, Arizona, 1982.
- [20] G. Blunden, A. Carabot, A.L. Cripps, K. Jewers, Ruizgenin, A new steroidal sapogenin diol from *Agave lechuguilla*, *Steroids* 35 (1980) 503–510.
- [21] K.J. Hong, S. Toknagen, Y. Ishigami, T. Kajiuchi, Extraction of heavy metals from MSW incinerator fly ash using saponins, *Chemosphere* 41 (2000) 345–352.
- [22] K. Hong, S. Tokunaga, T. Kajiuchi, Evaluation of remediation process with plant-derived biosurfactant for recovery of heavy metals from contaminated soils, *Chemosphere* 49 (2002) 379–387.
- [23] J. Romero-González, I. Cano-Rodríguez, J.C. Walton, J.R. Peralta-Videa, E. Rodríguez, J.L. Gardea-Torresdey, A model to describe the adsorption and reduction of Cr(VI) from an aqueous solution by *Agave lechuguilla* biomass, *Rev. Mex. Ing. Quím.* 4 (2006) 257–268.
- [24] B. Volesky, Biosorption process simulation tools, *Hydrometallurgy* 71 (2003) 179–190.
- [25] A.E. Rodríguez, Z.P. Lu, J.M. Laureiro, Residence time distribution of inert and linearly adsorbed species in a fixed bed containing pore support: applications separation engineering, *Chem. Eng. Sci.* 46 (1991) 2765–2773.
- [26] K. Vijayaraghavan, D. Prabu, Potential of *Sargassum wightii* biomass for copper(II) removal from aqueous solutions: application of different mathematical models to batch and continuous biosorption data, *J. Hazard. Mater.* 137 (2006) 558–564.
- [27] M. Ramirez, M. Pereira, S.G. Ferreira, O. Vasco, Mathematical models applied to the Cr(III) and Cr(VI) breakthrough curves, *J. Hazard. Mater.* 146 (2007) 86–90.
- [28] C.E. Borba, E.A. Silva, M.R. Fagundes-Klen, A.D. Kroumov, R. Guirardello, Prediction of the copper (II) ions dynamic removal from a medium by using mathematical models with analytical solution, *J. Hazard. Mater.* 152 (2008) 366–372.
- [29] C.M. Chang, M.K. Wang, T.W. Chang, C. Lin, Y.R. Chen, Transport modeling of copper and cadmium with linear and nonlinear retardation factors, *Chemosphere* 43 (2001) 1133–1139.
- [30] S.K. Kamra, B. Lennartz, M.Th. Van Genuchten, P. Widmoser, Evaluating non-equilibrium solute transport in small soil columns, *J. Contam. Hydrol.* 48 (2001) 189–212.
- [31] A.M. Hamed, Theoretical and experimental study on the transient adsorption characteristics of a vertical packed porous bed, *Renew. Energy* 27 (2002) 525–541.
- [32] F. Sugita, R.W. Gillham, Pore scale variation in retardation factor as a cause of non-ideal reactive breakthrough curves I. Conceptual model and its evaluation, *Water Res.* 31 (1995) 103–112.
- [33] G. Naja, B. Volesky, Behavior of the mass transfer zone in a biosorption column, *Environ. Sci. Technol.* 40 (2006) 3996–4003.
- [34] G. Bohart, E.Q. Adams, Some aspects of the behaviour of charcoal with respect to chlorine, *J. Am. Chem. Soc.* 42 (1920) 523–544.
- [35] R.M. Clark, Evaluating the cost and performance of field-scale granular activated carbon systems, *Environ. Sci. Technol.* 21 (1987) 573–580.
- [36] D.J. Gunn, R. England, Dispersion and diffusion in bed of porous particles, *Chem. Eng. Sci.* 26 (1971) 1413–1423.
- [37] T. Miyauchi, T. Kikuchi, Axial dispersion in packed beds, *Chem. Eng. Sci.* 30 (1975) 343–348.
- [38] M.Th. van Genuchten, Convective-dispersive transport of solutes involved in sequential first-order decay reactions, *Comput. Geosci.* 11 (1985) 129–147.
- [39] J.J.A. van Kooten, A method to solve the advection-dispersion equation with a kinetic adsorption isotherm, *Adv. Water Res.* 19 (1996) 193–206.
- [40] B. Ataie-Ashtiani, D.A. Lockington, R.E. Volker, Truncation error in finite difference models for solute transport equation with first-order reaction, *J. Contam. Hydrol.* 35 (1999) 409–428.
- [41] V. Ravindran, B.N. Badriyha, M. Pirbazzari, S. Kim, Modeling of bioactive carbon adsorbents: a hybrid weighted residual-finite difference numerical technique, *Appl. Math. Comput.* 76 (1996) 99–131.
- [42] M.A. Hossain, M.E. Barber, Optimized Petrov-Galerkin model for advective-dispersive transport, *Appl. Math. Comput.* 115 (2000) 1–10.
- [43] M.A. Hossain, M.R. Taha, Simulating advective transport by finite elements criteria for accuracy of an explicit Runge-Kutta method, *Appl. Math. Comput.* 112 (2000) 309–316.
- [44] M.Th. van Genuchten, Analytical solutions for chemical transport with simultaneous adsorption, zero-order production and first-order decay, *J. Hydrol.* 49 (1981) 213–233.
- [45] B. Niemeier, T. Feilenreiter, H. Tiltscher, Theoretical studies on biospecific adsorption for large-scale affinity separations, *Chem. Eng. Sci.* 51 (1996) 5263–5271.
- [46] S.E. Bailey, T.J. Olin, R.M. Bricka, D.D. Adrian, A review of potentially low-cost sorbents for heavy metals, *Water Res.* 33 (1999) 2469–2479.
- [47] L. Sánchez, E. Romero, A. Peña, Ability of biosolids and a cationic surfactant to modify methidathion leaching. Modelling with pescol, *Chemosphere* 53 (2003) 843–850.
- [48] Y.H. Huang, T.C. Zhang, Modeling of nitrate adsorption in Fe⁰-packed columns through impulse loading tests, *J. Environ. Eng.* 131 (2005) 1194–1202.
- [49] M. Hauns, P.Y. Jeannin, O. Atteia, Dispersion, retardation and scale effect in tracer breakthrough curves in karst conduits, *J. Hydrol.* 241 (2001) 177–193.
- [50] J.L. Gardea-Torresdey, K.J. Tiemann, V. Armendáriz, L. Bess-Oberto, R.R. Chianelli, J. Rios, J.G. Parsons, G. Gamez, Characterization of Cr(VI) binding and reduction to Cr(III) by the agricultural byproducts of *Avena monida* (Oat) biomass, *J. Hazard. Mater.* B80 (2000) 175–188.
- [51] J.G. Parsons, M. Hejazi, K.J. Tiemann, J. Henning, J.L. Gardea-Torresdey, An XAS study of the binding of copper(II), zinc(II), chromium(III) and chromium(VI) to hops biomass, *Microchem. J.* 71 (2002) 211–219.